

Original Research

Spatio-Temporal Variations of Water Quality and Planktonic Algal Communities in Qingshan Reservoir, China

Yan Yan^{1#}, Zhenbo Xu^{1,2,3#}, Bingxue Yang³, Niwen Jiang^{1,2}, Shengjia He^{1,4*}, Hanjiao Sheng⁵, Weijun Fu^{1,2}

¹College of Environmental and Resource Sciences, Zhejiang A&F University, Lin'an 311300, China

²Key Laboratory of Soil Contamination Bioremediation of Zhejiang Province, Zhejiang A&F University, Lin'an 311300, China

³Ecological Environmental Monitoring Station, Lin'an, Hangzhou 311300, China

⁴State Key Laboratory of Subtropical Silviculture, Zhejiang A&F University, Lin'an, Hangzhou 311300, China

⁵Shixing Testing Co.LTD, Lin'an, Hangzhou 311300, China

Received: 15 June 2022

Accepted: 3 January 2023

Abstract

Based on the monitoring data of conventional water quality in Qingshan Reservoir from 2018 to 2019, principal component analysis (PCA) and comprehensive nutritional status index (TLI) are used to evaluate water quality, planktonic algal communities, and eutrophication degree of Qingshan reservoir. The results showed that: 1) from 2018 to 2019, the annual average TLI is 56.54, indicating that the reservoir is in a slightly eutrophic state, which is conducive to algae growth; 2) the water quality of Qingshan Reservoir has obvious temporal and spatial variability: the water environment quality commonly decreased in the order winter>spring>autumn>summer, and exit zone>buffer zone>entry zone; meanwhile, the algal biomass in summer and autumn was significantly higher than that in spring and winter, and most of the algae were concentrated in the surface water except in January and decreased with the increase of depth; And related to the water quality environment, the biomass of cyanobacteria and green algae in Qingshan Reservoir is relatively high in summer, while diatom is the dominant species in spring and winter. We come to the conclusion that targeting at region and time will be more effective for the treatment of reservoir eutrophication.

Keywords: eutrophication, non-point source pollution, spatio-temporal variations, water quality, planktonic algal communities, Qingshan Reservoir

[#]These authors contributed equally to this work and should be considered co-first authors.

*e-mail: hesj86@sina.cn

Introduction

With the rapid development of the economy and the acceleration of urbanization, the problems of water shortage and water pollution are on the rise [2, 3]. Lakes and reservoirs, accounting for about 0.3% of the total surface waters, are important sources of water supply for human life, generally [4, 5], and they also play a vital role in providing drinking water, flood control, agricultural irrigation, aquaculture, and wetland ecosystem protection [6]. As point-source pollution control has been well-controlled in recent years, agricultural non-point source pollution has become the main pollution source of surface waters [7]. In Europe, nearly 15~34% of TP (total phosphorus) loss and 50% of the TN (total nitrogen) loss were contributed by the agricultural sources [8]. That excessive nitrogen (N) and phosphorus (P) entering the water body will lead to water eutrophication. Therefore, eutrophication caused by agricultural non-point source pollution has become the main water environment problem of reservoirs and lakes presently [9].

Eutrophication, a common water pollution phenomenon, is mainly manifested in increasing the concentration of nutrients such as N and P, aggravating the consumption of dissolved oxygen (DO), destroying the original oxygen balance in the water, and causing suffocation and death of aquatic animals [10], producing algal toxins and endangering human health [11], generating peculiar smell, affecting the water landscape and the development of aquaculture [12]; influencing water purification process [13], etc. Globally, 30%~40% of lakes and reservoirs are affected by eutrophication in varying degrees. Among the 96 lakes monitored in Europe, 80% are polluted by N and P, presents a serious state of eutrophic; at least a third of Spain's 800 counted reservoirs are highly eutrophic; of the 493 lakes monitored in the United States, the proportion of eutrophication is as high as 76% [14]. In China, nearly 30% of reservoirs and lakes are in different degrees of eutrophication pollution [15]. It leads to the deterioration of physical and chemical indexes of water bodies, the change of algae community composition and structure, the deterioration of water quality, and the damage of ecosystem and water function [16, 17].

The average concentration-based methods are commonly not consummate for eutrophication evaluation because the non-point source nutrient pollutants (e.g., TN and TP) discharged into the waters will not only fluctuate greatly with different water regimes due to seasonal changes [18, 19] but also show great spatial variability due to the impact of the surrounding environment of lakes and reservoirs [1, 20]. The distribution of nutrients in lakes and reservoirs [21] and the differences of environmental factors such as water temperature [22] and pH [23] will further affect the composition and distribution of planktonic algae community [24]. Therefore, studying and analyzing the spatio-temporal distribution characteristics of the

water quality and planktonic algal communities in the reservoir is an important basis for obtaining the water environment information, evaluating its water environment quality, exploring its main pollution sources, and carrying out the effective treatment of non-point source pollution in the lake and reservoir [8, 20].

The main objectives of this study were to 1) examine the spatio-temporal variation of water quality and planktonic algae in the Qingshan Reservoir (Southeast China); 2) to assess the eutrophication status of the reservoir using a comprehensive nutritional status index (TLI); 3) explore the relationship between the spatio-temporal variation of the water quality and planktonic algal to supply theoretic and data support for the treatment of lake and reservoir non-point source pollution in the future.

Materials and Methods

Study Area

Qingshan Reservoir (119°75'79"–119°81'83"E and 30°21'94"–30°25'99"N) is located in the middle-lower reaches of South Tiaoxi River, Zhejiang Province, Southeast China (Fig. 1), and it belongs to Taihu Lake Basin. The rainwater catchment area of the reservoir is 603 km² with the main source length is 46 km, and the total storage capacity is 2.15×10⁸ m³. The soil at the bottom of the reservoir is mainly sediment. The reservoir is in the central subtropical monsoon climate zone with four distinct seasons, spring and summer account for 70% of the annual rainfall. Qingshan Reservoir is one of the three major drinking water sources in Hangzhou. About 1.5 million people in Hangzhou draw 6.2×10⁵ tons of water every day. It shows remarkable social and economic efficiency. In recent years, Qingshan Reservoir faces eutrophication, phytoplankton bloom appearance, and water quality deterioration risk, which threaten drinking water supply safety.

Sample Collection and Analysis

Water samples were collected monthly at 10 sampling points (Fig. 1) from April 2018 to March 2019. All the water samples were collected approximately 50 cm below the water surface in 2.5-L polyethylene bottles and immediately transported to the laboratory and stored at 4°C before analysis. The water quality parameters, including pH, dissolved oxygen (DO), potassium permanganate index (COD_{Mn}), ammonia nitrogen (NH₄-N), total nitrogen (TN), manganese (Mn), electrical conductivity (EC), total phosphorus (TP), and inorganic dissolved phosphorus (PO₄-P) were measured by standard methods [25]. In addition, the sampling point in the center of the lake (No. 4 in Fig. 1) was selected to monitor the vertical distribution of algae. The density of chlorophyll a (Chl-a), green

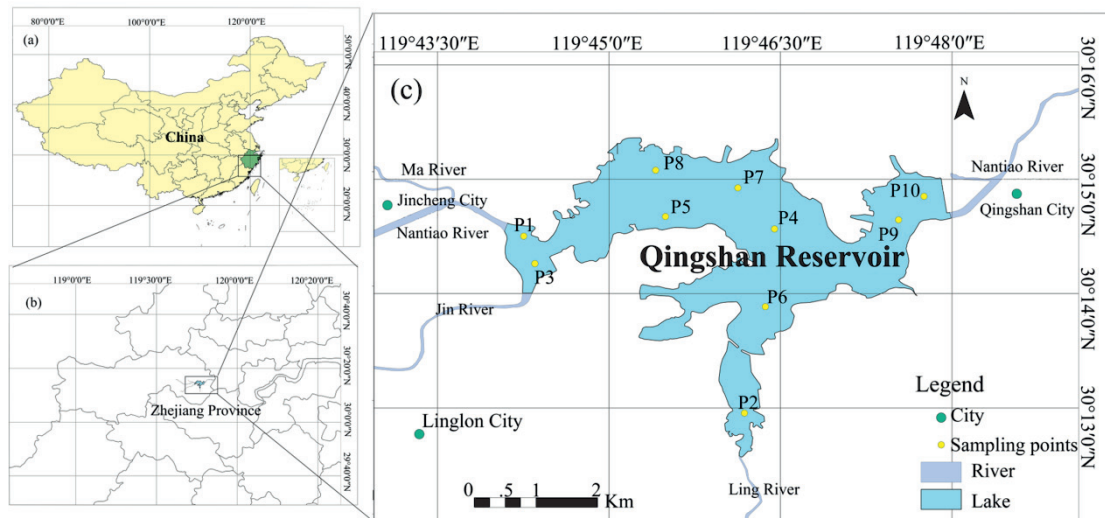


Fig. 1 Sampling points in Qingshan Reservoir.

algae, cyanobacteria, and diatom were determined by fluorescence spectrometry [26].

Statistical Analyses and Eutrophication Assessment

Principal component analysis (PCA) is used to provide an objective way to explain the contribution of different water quality indexes to water quality so that the variation in the data can be accounted for as concisely as possible [27]. The score calculation formula of each principal component can be expressed as:

$$F_i \sum_{k=1}^n a_{ik} Z_j \quad (1)$$

where F_i is the score of PCs, a_{ij} is the factor loading, Z_j is the normalized value of the original data; 1, 2, ..., m ; 1, 2, ..., n ; $m < n$.

The comprehensive score formula of the principal component is:

$$F = \sum_{k=1}^n e_i F_i \quad (2)$$

where F is the total score, e_i is the contribution rate of its principal component; 1, 2, ..., m .

The eutrophication degree of lakes and reservoirs was assessed by using the comprehensive nutritional status index method (TLI) [28], the calculation of the comprehensive nutrient status index is as follows:

$$TLI(\Sigma) = \sum_{j=1}^m W_j \cdot TLI(j) \quad (3)$$

where, TLI is the sum of indexes of all nutrient parameters, $TLI(j)$ is the TLI of j parameter, W_j is the proportion of j parameter in the TLI , m is the number of evaluation parameters.

Results and Discussion

Spatial Heterogeneity of Water Quality

In PCA, the higher the composite score of the sample, the greater the variance contribution rate of the index and the greater the influence of the sample on the overall data [29]. Therefore, in the water quality evaluation, the higher the comprehensive score is, the higher the content of pollutants and elements in the sample is, and the worse the water quality is. The principal component load matrix (Table 1) indicates that the PC with a high degree of interpretation mainly reflects the water quality information including organic pollution indicators, including COD_{Mn} , NH_4-N , TN, and Chl-a. Kaiser Meyer Olkin (KMO) and Bartlett's sphericity test is used to testing the applicability of the data [30]. The results show that the KMO value is 0.59 (spatial), and the significance level is less than 0.05. Three PCs in space were extracted from various water quality indexes of Qingshan Reservoir, with the cumulative contribution rate reaching 90.55%.

At space scale, the comprehensive scores of each sampling point were $P6 > P2 > P5 > P1 > P7 > P8 > P4 > P3 > P9 > P10$. Kriging interpolation results showed NH_4-N , COD_{Mn} , Chl-a, with exit zone < buffer zone < entry zone (Fig. 2). NH_4-N undergoes various reactions in water, and the concentration gradually decreases in the order of the entry area > buffer area > exit area. The main reasons for this phenomenon can be summarized as: 1) the upstream carries a large amount of agricultural and industrial wastewater into Qingshan Lake, leading to a high concentration of NH_4-N at the entrance; 2) the longer retention time due to the lower flow rate led to the rapid decomposition of NH_4-N in the buffer zone and the reduced concentration [31]; 3) the lowest concentration in the exit zone may be due to the adsorption and decomposition of algae and plants [32], nitrification of bacteria [33], mineralization back to the organism [34]

Table 1. Principal component load matrix of Qingshan Reservoir water quality index.

Indicators	Component		
	1	2	3
Ttemporal			
pH	0.41	0.10	
DO	0.22	0.52	
COD _{Mn}	0.35	-0.24	
NH ₄ -N	-0.39	0.09	
TN	-0.30	0.45	
EC	0.04	0.48	
PO ₄ ³ P	-0.30	-0.44	
Mn	-0.41	-0.01	
Chl-a	0.40	-0.14	
Spatial			
pH	-0.40	-0.15	0.22
DO	-0.44	0.08	-0.20
COD _{Mn}	0.05	0.58	-0.11
NH ₄ -N	0.14	-0.15	0.75
TN	-0.16	-0.08	0.81
EC	0.30	0.26	-0.56
PO ₄ ³ P	0.45	0.04	-0.08
Mn	0.12	-0.55	0.27
Chl-a	0.14	0.57	-0.12

in the buffer zone. Generally, the water quality flowed out of the studied reservoir area was the best, followed by the buffer zone, and the entry zone was the worst. Investigation showed that Qingshan Reservoir's main inflow surface runoff included South Tiaoxi River, Jinxi River, and Lingxi River, etc. The upstream is Lin'an City, which is greatly affected by human activities, further adding to the pollution emissions. From west to east, the South Tiaoxi River is surrounded by a chunk of farmland. Affected by the discharge of wastewater and sewage treatment plants along the way, the content of organic and inorganic substances in the water body has greatly increased. Moreover, the slope of Qingshan Reservoir is high in the west and low in the east, thus, pollutants are easy to accumulate in the entrance area. After entering Qingshan Reservoir, the water quality fluctuated, indicating that Qingshan Reservoir, as an ecological reservoir, had a certain function of improving water quality.

The eutrophication evaluation results of Qingshan Reservoir showed that the concentration of various water quality indicators in the entry zone was basically higher than that in other areas of the reservoir, indicating that the pollutants in Qingshan Reservoir mainly come from the outside. The upstream river of Qingshan Reservoir carries a large number of pollutants, which aggravates the pollution load of N and P in the reservoir. The upstream is the main urban area of Lin'an City. The discharge of domestic sewage, agricultural wastewater by massive numbers of people further increases the pollution emission, making the pollutant input situation in the entry zone more severe [35].

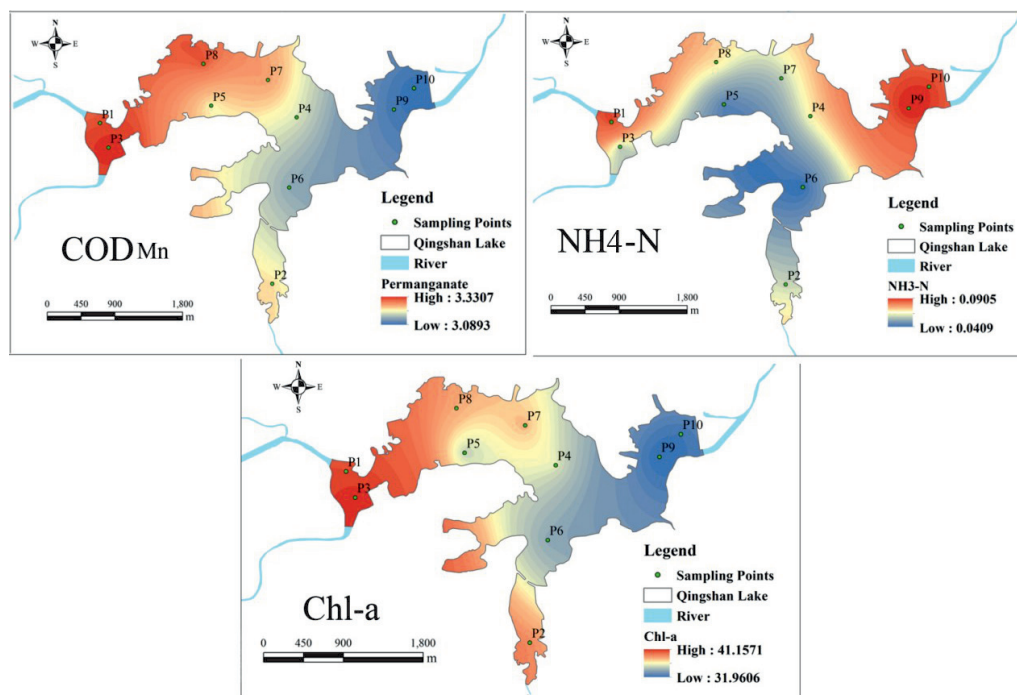


Fig. 2 Spatial heterogeneity of COD_{Mn}, NH₃-N, Chl-a in Qingshan Reservoir.

Table 2. Class III limited value (China water quality standard) of main water quality indicators.

Class III Limited value	Indicators					
	pH	DO	COD _{Mn}	NH ₄ -N	TN	TP
	6-9	≥5	≤6	≤1	≤1	≤0.05

Time Heterogeneity of Water Quality

During the study period (April 2018 to March 2019), except for TN and TP, other water quality indicators of Qingshan Reservoir all met the standard limited value (Table 2). The pH value of Qingshan Reservoir exceeded the standard (the pH limit is 6-9) in May, July and September. The concentrations of DO, COD_{Mn} and NH₄-N (mg/L) weren't exceeded, and the over standard rate was 0%. The average concentrations of TN and TP during the study period were 0.08 and 2.95 respectively, which exceeded their corresponding limit (0.05 and 1.0 respectively), 60% and 195% higher than the upper limit of reservoir water quality standards (Fig. 3).

In order to study the temporal heterogeneity of water quality in Qingshan Reservoir, two PCs were extracted at time scale based on common parameters (e.g., pH, TN, and TP, etc.), and the cumulative contribution rate of this two PCs reached 82.34% (KMO = 0.57, $p < 0.05$). In terms of time, the water quality parameters of Qingshan Reservoir have obviously seasonal changing regularities (Table 3). The average value was higher in summer and lower in

winter. The water quality was ranked as winter>autumn>spring>summer. This phenomenon is closely related to water temperature because DO saturation increases under high temperatures. In addition, summer is the rainy season, with large rainfall and rapid water flow, which promotes the rise of DO concentration [36]. This provides favorable environmental conditions for the growth of algae, resulting in a significant increase in Chl-a concentration in water and serious deterioration of water quality [37].

In addition, the test results of many water quality indicators showed that the content in winter and spring were higher than that in summer and autumn, especially the concentration of TN, which was the lowest in summer and highest in winter and spring (Fig. 4). This phenomenon might be related to the hydrological conditions of Qingshan Reservoir Basin. The precipitation of Qingshan Reservoir varies greatly in different seasons, and about 70% of the precipitation is concentrated in summer and autumn, in which a large amount of rainfall makes the water quality purified to a certain extent. In addition, the algae grows in summer can also lead to the high consumption

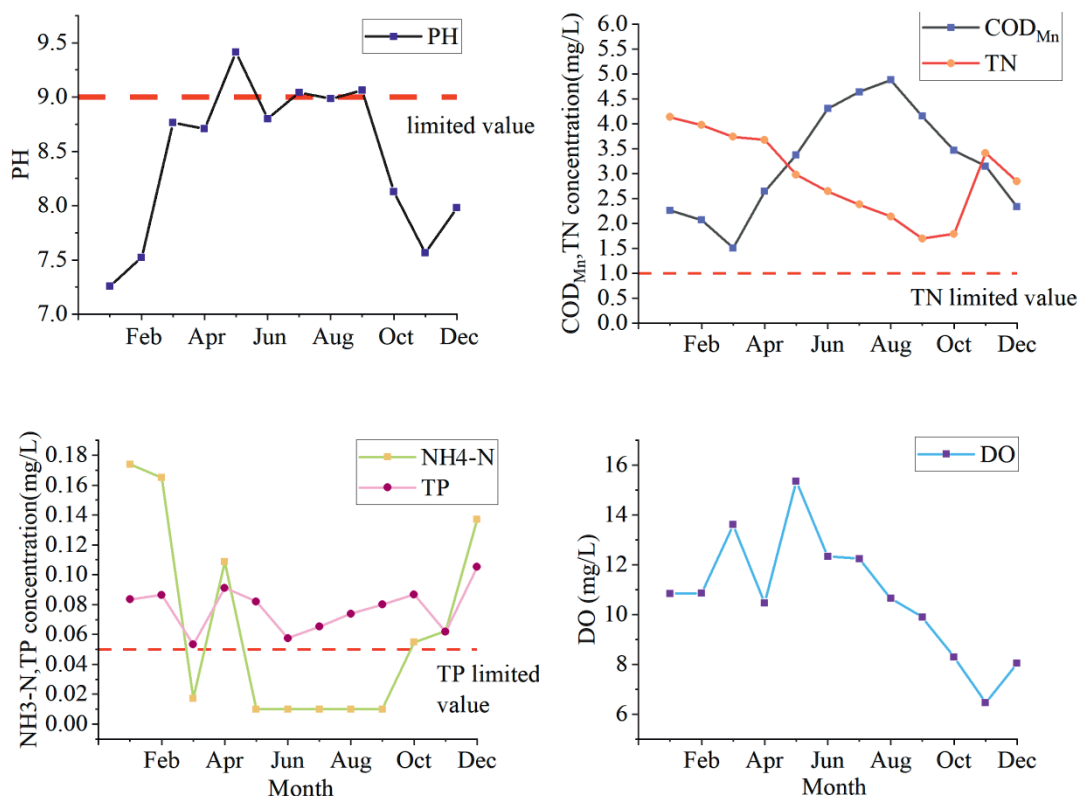


Fig. 3 Water quality monitoring results of Qingshan Reservoir.

Table 3. Spatio-temporal comprehensive score of water quality index of Qingshan Reservoir.

Temporal Season	F1	F2	F (composite)	Rank	
Spring	0.528	1.602	0.855	2	
Summer	2.487	-0.008	1.727	1	
Autumn	-0.168	-1.789	-0.662	3	
Winter	-2.848	0.195	-1.921	4	
Spatial					
No.	F1	F2	F3	F (composite)	Rank
P1	0.892	-2.761	3.420	0.130	4
P2	2.752	1.437	-3.356	1.352	2
P3	-0.526	-2.745	2.935	-0.680	8
P4	-1.250	0.996	0.287	-0.285	7
P5	-0.110	-0.268	1.923	0.166	3
P6	2.491	3.398	-2.935	1.911	1
P7	-1.187	1.359	-0.390	-0.245	5
P8	-0.830	0.453	0.241	-0.248	6
P9	-0.833	-0.999	-0.894	-0.248	9
P10	-1.400	-0.870	-1.232	-1.204	10

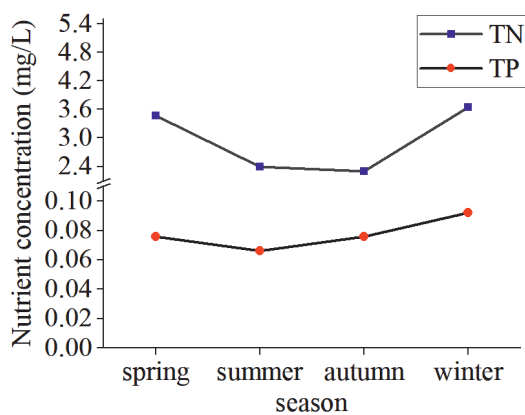


Fig. 4 Variations of TN and TP concentrations in Qingshan Reservoir.

of N and P nutrients. [38, 39], and thus the index concentration decreases. At the same time, there are vast areas of farmland around Qingshan Reservoir. Due to insufficient rainfall in winter, reservoir water is often used for irrigation. Improper irrigation and drainage methods will make pesticides enter the reservoir and increase relevant indicators.

Eutrophication Condition of the Reservoir

As agricultural production, soil and water loss and atmospheric sedimentation are the causes of non-

point source pollution [9], several non-point source related indexes (e.g., Chl-a, TN, TP, COD_{Mn} and SD, etc.) were selected to analyze the eutrophication of Qingshan Reservoir. $\text{NH}_4\text{-N}$, TN, and Chl-a are the main indicators of water eutrophication. According to the monitoring data from April 2018 to March 2019, the comprehensive eutrophication index of Qingshan Reservoir in different seasons was calculated. As shown in Fig. 5, the TLI in spring, summer, autumn, and winter were 57.28, 59.73, 57.03, and 52.10 respectively. The TLI value was the highest in summer and lowest in winter. Referring to the regulations on assessment methods and classification technology of Lake (reservoir) eutrophication [30] issued by China Environmental Monitoring Station (csemz) [2001] No. 90, $50 < \text{TLI} < 60$ indicates mild eutrophication, $60 < \text{TLI} < 70$ indicates moderate eutrophication, and $\text{TLI} > 70$ indicates severe eutrophication [40]. Therefore, Qingshan Reservoir was in the state of mild eutrophication of the whole lake, and had obviously trend towards moderate eutrophication.

The evaluation results based on TLI showed that the water quality of Qingshan Reservoir was poor in recent years. Among them, the main excessive substances were nitrogen, phosphorus nutrients. The ratio of nitrogen to phosphorus is often used to evaluate eutrophication [41]. During the monitoring period (April 2018 to March 2019), the annual average concentration of TN and TP in Qingshan Reservoir were 2.95 mg/L and 0.08 mg/L, both higher than the limit value. The structure of the algal community has a strong response

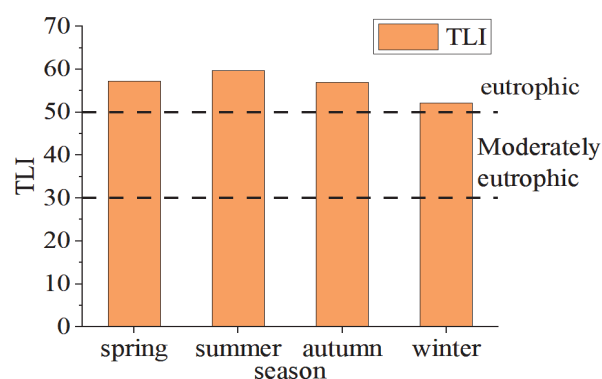


Fig. 5 Variations of TLI in Qingshan Reservoir.

to the N:P ratio and total nutrient concentration. N:P ratio required for healthy growth and physiological balance of plankton algae is 16:1. TP is the limiting factor for algae growth when the specific value is higher than 16:1, while it's TN if less than 16:1 [42]. The annual N: P values of Qingshan Reservoir were between 21.21 and 70.28, which were higher than 16, and indicated that TP was the main limiting factor of reservoir eutrophication. The monitoring data showed that the N: P ratio in winter and spring was higher than that in summer, which reflected the seasonal character pattern driven by the asynchronous dynamics of TN and TP in Qingshan Reservoir [43]. Schindler [44] pointed out that cyanobacteria bloom will reduce the mass concentration of N, increase the mass concentration of P and reduce the ratio of N: P. Therefore, the flowering of cyanobacteria in summer may be the reason for the low N: P in summer. Attention should be paid to monitoring the changes of water quality in summer and the prevention and control of cyanobacteria bloom, and the phosphorus input of Qingshan Reservoir should be putting in the first place.

Spatio-Temporal and Vertical Variation of Planktonic Algae

Spatio-Temporal Variation of Planktonic Algae

Compared with rivers, the reservoir has the characteristics of slow water flow and a larger still water area, which provided good conditions for the growth of

algae [4, 45]. Algae usually contain a variety of pigment components, and Chl-a exist in various algae. Therefore, Chl-a is usually used to characterize the biomass of algae in aquatic ecosystems [46]. From the perspective of spatial sampling points, the horizontal change of the algal biomass composition of Qingshan Reservoir was shown in Fig. 6. The algal biomass of P4 and P7 in the buffer zone of the reservoir was high, with an annual average of 38.83 $\mu\text{g/L}$, and the algal biomass of P5 and P6 was low. The average algae biomass in the entry zone and exit zone of the reservoir were 41.26 $\mu\text{g/L}$ and 29.92 $\mu\text{g/L}$ respectively. According to the horizontal distribution of algae, the average density of algae in the entry area (5, 6), buffer area (1, 3, 4, 7, and 8), and exit area (2, 9 and 10) of Qingshan Reservoir were 6.78, 7.82, and 6.36 cells/L respectively. According to the correlation analysis between phytoplankton and environmental factors (Table 4), algae biomass and functional community were significantly correlated with water temperature ($p < 0.01$), indicating that the fluctuation of water temperature had a great impact on the growth of algae. Studies have shown that phytoplankton adapted to temperature changes through changes in chlorophyll productivity and cell division rate, and the range of temperature changes is conducive to the increase of cell division rate and the growth of phytoplankton [47, 48]. The high temperature of the buffer zone usually associated with the slow flow speed and together with the long replacement cycle, and it was suitable for algae growth. Compared with other area, the water quality in the entry area was poor, and the concentration of COD_{Mn} and other substances was high, but was suitable for the growth of algae. After the buffering and purification of Qingshan Reservoir, the water quality in the exit area was improved to certain extent, and thus the algae biomass was the lowest due to the fast water exchange and low water temperature.

The horizontal distribution of different algae community compositions in Qingshan Reservoir from spring to winter is shown in Fig. 7. The total average density of all algae in the reservoir area was 7.22×10^6 cells/L, and the algae density in summer and autumn was absolutely dominant. The average value of algae density at each point was 11.75/L in spring, 46.74/L in summer, 23.91/L in autumn, and 4.20/L in winter respectively. The algae density in the flood season was significantly higher than that in the dry

Table 4. Correlations between environmental factors and algae.

Indicators	Chl-a	pH	TN	TP	COD_{Mn}	DO	SD	WT	Green Algae	Cyanobacteria	Diatom
Chl-a	1	0.725**	-0.758**	-0.298	0.949**	0.251	0.282	0.941**	0.983**	0.952**	0.855**
Green Algae	0.983**	0.671*	-0.826**	-0.25	0.962**	0.162	0.269	0.938**	1	0.929**	0.784**
Cyanobacteria	0.952**	0.565	-0.728**	-0.324	0.907**	0.117	0.315	0.819**	0.929**	1	0.726**
Diatom	0.855**	0.812**	-0.551	-0.26	0.742**	0.443	0.318	0.863**	0.784**	0.726**	1

Significant correlation at the * $P < 0.05$ and ** $P < 0.01$ levels

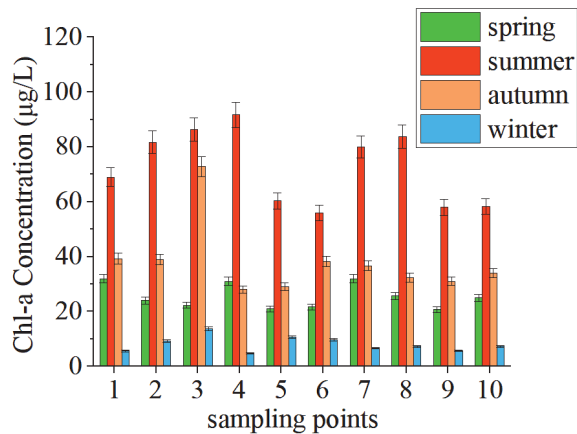


Fig. 6 Horizontal variations of algal biomass (with chlorophyll a concentration) composition in Qingshan Reservoir.

season. In the same sampling area, the algae biomass in winter was the lowest, with an average of 8.07 mg/L, which was clearly lower than that in summer and autumn. Algae biomass was highest in summer, with an average of 72.50 mg/L; The algae biomass in autumn was higher than that in spring, with an average value of 38.05 mg/L and 25.40 mg/L respectively (Fig. 7). It is mainly due to the influence of temperature and light. From November to January of the next year, the temperature was low and the light conditions were poor, which was not suitable for the occurrence of a

series of biological activities such as algae reproduction and photosynthesis. After February, the temperature gradually warmed up, around August, the water temperature was maintained at a very favorable level for algal growth and the light is abundant. At this time, the risk of algal bloom is also the maximum.

In view of the composition of algae population structure, the density of diatom was the highest in spring and winter, accounting for 48% and 52% of the total seasonal algae density respectively, and the density of green algae and cyanobacteria is relatively low. The composition of algae at each point is basically the same in spring and winter, with the highest density of diatom, followed by green algae and cyanobacteria. In summer and autumn, on the contrary, cyanobacteria and green algae replaced diatoms as dominant species. Especially in summer, cyanobacteria grow vigorously, and the population proportion is as high as 50%. The density of cyanobacteria was the highest in summer and autumn, followed by green algae, and the density of diatom was the lowest. In spring and winter, diatoms become dominant species because diatoms are more suitable for growth and reproduction at low temperatures [49, 50]. Sommer studied the growth characteristics of large numbers of phytoplankton in temperate lakes, proposed a PEG (phytoplankton ecological group) model, and pointed out that the succession law of phytoplankton is mainly diatom in winter and spring and green algae in summer. Until late summer and early autumn, cyanobacteria dominated, and in late autumn, diatoms became the dominant

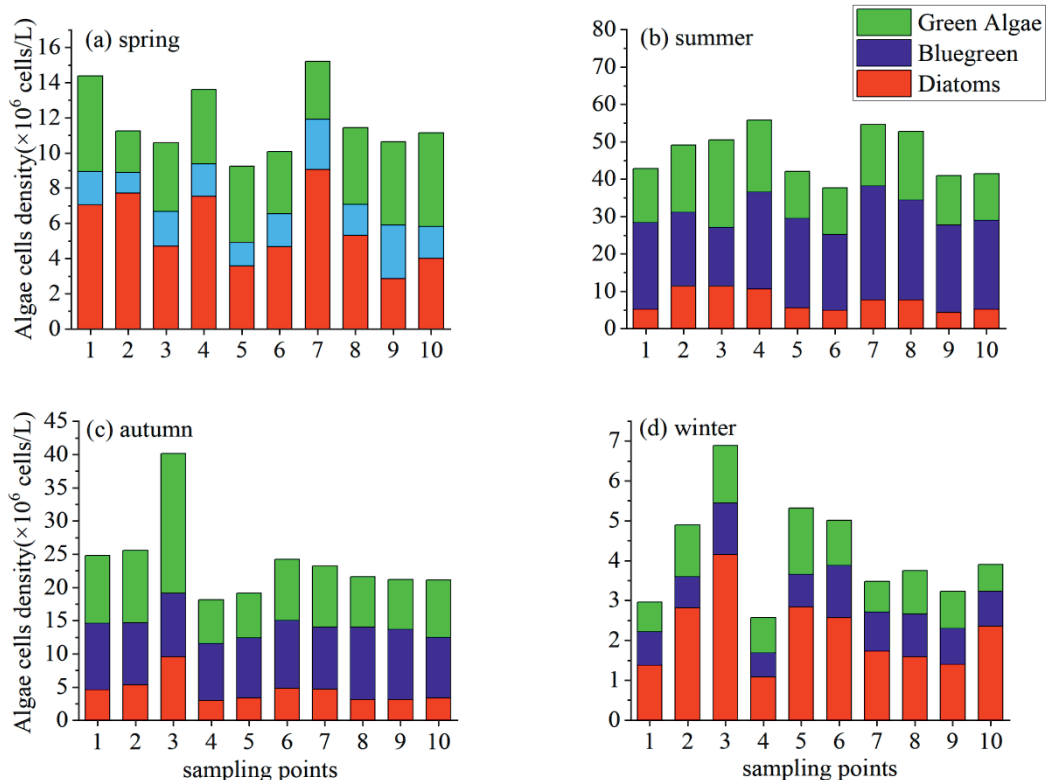


Fig. 7 Horizontal variations of algal community composition in the Qingshan Reservoir.

species again. In this study, the seasonal composition of the algal community conforms to the model [51].

Vertical Variation of Planktonic Algae

In order to explore the seasonal vertical distribution characteristics of algae in Qingshan Reservoir, the lake center point (No. 4, Fig. 1) is selected, and the vertical distribution maps of algae density in January, May, August and November were drawn according to the test results. In January (Fig. 8a), three algae biomass had risen with the increase of depth, of which diatom increased the most. Different from January, three kinds of algae biomass increased first and then decreased, and most of them were concentrated on the surface water body (1-3 m underwater) in May, August, and November (Fig. 8(b-d)). In May, the peak density of green algae and diatom appeared at the depth of 1.9 m, and the peak density of cyanobacteria appeared at the depth of 2.4 m, reaching 18.30 cells/L, 17.62 cells/L and 15.00 cells/L respectively. After that, the number of algae decreased rapidly. In August, the peak values of the three algae at 0.7m depth were 26.61 cells/L, 22.79 cells/L and 16.72 cells/L respectively. Compared with May, algae decreased less with depth in August. In November, various algae appeared multiple peaks in the distribution of 0-3 m water depth. With the slow decline of water depth, the peak increased slightly, and then with the decrease of water depth, the algae density changed little. The density of green algae was the highest, followed by cyanobacteria, and diatom was the lowest.

The change of algae growth in the vertical direction is closely related to temperature [52]. There are apparent changes of plankton absorption rate in different seasons, due to the stratification in waters that caused by the variations of temperature. In general, the higher the temperature is, the stronger the absorption rate is [20]. This indicates that plankton biomass generally reaches a peak in summer and autumn, when the water temperature is relatively high [53]. In this study, the algae biomass of the Qingshan Reservoir was significantly correlated with the water temperature ($r = 0.943$, $p < 0.01$). At monthly scale, for example, the highest (27008 cells/mL) and lowest (5325 cells/mL) average algal biomass in the Qingshan Reservoir were observed in the the August and January, respectively, which represented the highest (29.46°C) and lowest (7.42°C) monthly mean temperature, respectively. In the same period, such as May, the correlation coefficient between algae biomass and temperature was up to 0.878 ($p < 0.01$). Above all, the change of water environment temperature strongly affects the biological response of algae [54].

Previous studies have shown that algae growth is closely related to light, and the reduction of light leads to the decrease of algae biomass [55, 56]. Such kind of phenomenon was also observed in the Qingshan Reservoir. Taking November as an example, the calculated correlation coefficient between algal biomass and depth went up to 0.973. Overall, most algae of the Qingshan Reservoir were distributed in the water surface to 3 m depth, and the biomass of these algae decreased with the increase of depth.

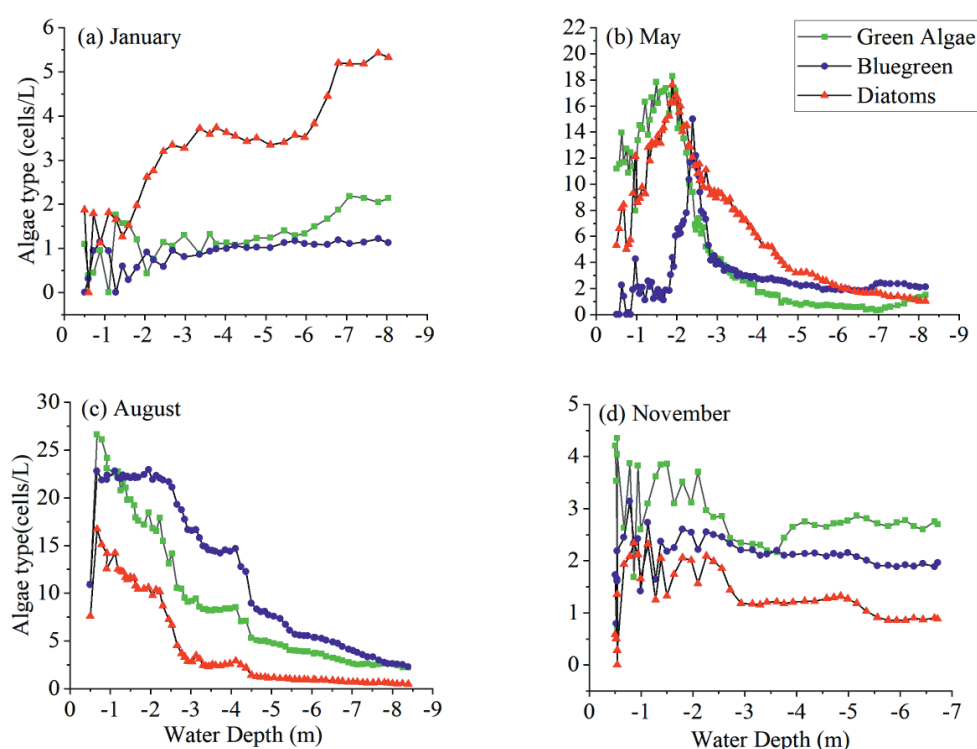


Fig. 8 Vertical variations of algal community in the Qingshan Reservoir.

The average algal biomass in the surface layer (1-3 m) was 6919.26 cells/mL. The average algal biomass in the deep water was 5758.86 cells/mL, and the surface water was 20.15 % higher than the deep water.

In terms of the horizontal distribution of algae, the distribution of phytoplankton in each part of the reservoir in the same period is generally shown as entry area>buffer area>exit area. There was no significant difference in algal biomass and species composition at each sampling point. It is speculated that Qingshan Reservoir is a large artificial lake, owing to the evaporation and heat transfer, the lake water temperature difference decreases during the formation process [57], which may also be related to the layout of sampling points or lake structure.

Organic pollutants provide nutrients for algae growth. Algae biomass in the surface water is closely associated with the concentration of COD_{Mn} , which is considered to be one of the representative of organic pollutants [58]. It is reported that algae biomass would increase with the increase of COD_{Mn} concentration within a certain range [59]. As expected, significant positive correlation ($r = 0.949$, $p < 0.01$) was obtained between the COD_{Mn} concentrations and the algae biomass. Moreover, the algae biomass of the Qingshan Reservoir was also significantly correlated ($r = 0.725$, $p < 0.01$) with the values of pH in the water, which usually varied from 7.26 to 9.41. For algal organisms, cyanobacteria, green algae and other algae that are prone to cause blooms are more suitable for weak alkaline environment [60]. Therefore, the acid-base conditions of Qingshan Reservoir also create a good environment for algae breeding. Fig. 9 shows the seasonal variation of algal biomass with depth at point 4, which is represented by Chl-a. Since the temperature increased in March, the algal biomass increased significantly, reaching the highest value of 96.70 $\mu\text{g/L}$ in July. After November, the change of algal biomass with depth was not obvious, and with the continuous decrease of temperature, the number of algal organisms showed an upward trend, which was consistent with the change trend of algal density in Fig. 7. In conclusion, algal growth has changed significantly over time. According

to the correlation analysis in Table 4, the correlation between algae biomass and water temperature is as high as 0.941. Since the water temperature changes with the temperature, the seasons and the rise and fall of the temperature must lead to the right water temperature. Therefore, controlling water quality factors has become the most critical method to prevent the occurrence of algal blooms in urban rivers. One of the most important is preventing algal blooms in urban rivers. Pre-outbreak bloom control must be achieved by preventing and controlling the main control factors in advance [61].

Conclusions

Because of the influence of anthropogenic activities or different natural conditions, Qingshan Reservoir showed obviously spatio-temporal variations features of water quality and planktonic algal communities, and the reservoir was in the mild eutrophication status based on the TLI value. To protect the water quality and beneficial uses of the reservoir, this study provides some suggestions: 1) planktonic algae can characterize the quality of water, thus, we can focus on the area where algae bloom to control the non-point pollution sources near the mass reproduction area. 2) Regular water quality monitoring should be conducted. 3) In addition, the results of this study reveal that analyzing water from the perspective of three-dimensional can provide efficient guarantee for water management and conservation of the reservoir.

Acknowledgments

This work was supported by the National Natural Science Foundation of China (Grant No. 42277045, 41807154), Natural Science Foundation of Zhejiang Province, China (Grant No. LY21D010001), and Key Research & Development Program of Zhejiang Province, China (2019C03121).

Conflict of Interest

The authors declare that they have no conflict of interest.

References

- GAO M., ZHU K., BI Y., HU Z. Spatiotemporal patterns of surface-suspended particulate matter in the Three Gorges Reservoir. *Environmental Science & Pollution Research*. **23** (4), 3569, **2016**.
- ADU., TUOYO J., KUMARASAMY., VELLAISAMY M. Assessing Non-Point Source Pollution Models: a Review. *Polish Journal of Environmental Studies*. **27** (5), 1913, **2018**.

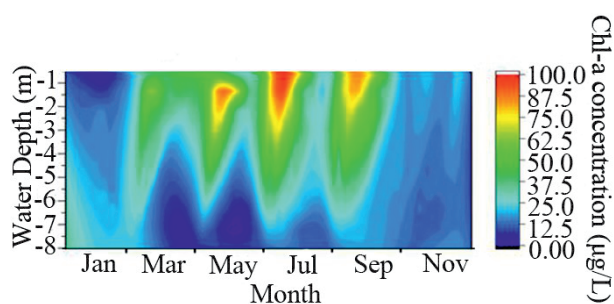


Fig. 9 Vertical variations of algal biomass (with chlorophyll a concentration) composition in the Qingshan Reservoir.

3. WANG H., XIONG J. Governance on water pollution: Evidence from a new river regulatory system of China. *Economic Modelling*. **113** (SI), 105878, **2022**.
4. CHENG X., CHEN L., SUN R., JING Y. Identification of regional water resource stress based on water quantity and quality: A case study in a rapid urbanization region of China. *Journal of Cleaner Production*. **209** (Feb.1), 2163, **2018**.
5. VASISTHA P., GANGULY R. Water quality assessment of natural lakes and its importance: An overview - ScienceDirect. *Materials Today: Proceedings*. **32** (4), 544, **2020**.
6. YANG X., CUI H., LIU X., WU Q., ZHANG H. Water pollution characteristics and analysis of Chaohu Lake basin by using different assessment methods. *Environmental Science and Pollution Research*. **27** (7), **2020**.
7. SRINIVAS R., SINGH AP., DHADSE K., GARG C. An evidence based integrated watershed modelling system to assess the impact of non-point source pollution in the riverine ecosystem. *Journal of Cleaner Production*. **246** (Feb.10), 118963.118961-118963.118917, **2020**.
8. AMA B., ME C., AS A., AAH C., AEA D., MF C. Evaluation of the water quality and the eutrophication risk in Mediterranean sea area: A case study of the Port Said Harbour, Egypt. *Environmental Challenges*. **7**, 100484, **2022**.
9. FU J., JIAN Y., WU Y., CHEN D., ZHOU F. Nationwide estimates of nitrogen and phosphorus losses via runoff from rice paddies using data-constrained model simulations. *Journal of Cleaner Production*. **279** (9), 123642, **2020**.
10. MAO Z., XIAOHONG GU., ZENG Q., ZHOU L., SUN M. Status and changes of fishery resources (2009-2010) in Lake Taihu and their responses to water eutrophication. *Journal of Lake Sciences*. **23** (6), 967, **2011**.
11. NOVELLI E., VALENTE J., RODRIGUES N.L. Toxic effects of water eutrophication on pancreatic, hepatic and osteogenic tissues of rats. *Toxicol Official Journal of the International Society on Toxinology*. **32** (10), 1270, **1994**.
12. JACOBSON P.C., HANSEN G., BETHKE BJ., CROSS T.K. Disentangling the effects of a century of eutrophication and climate warming on freshwater lake fish assemblages. *PLoS ONE*. **12** (8), e0182667, **2017**.
13. VAN GINKEL C. Eutrophication: Present reality and future challenges for South Africa. *Water Sa*. **37** (5), **2011**.
14. GILBERT P.M. Eutrophication, harmful algae and biodiversity – Challenging paradigms in a world of complex nutrient changes. *Marine Pollution Bulletin*. **124** (2), 591, **2017**.
15. SEPA 2020 China Environmental Bulletins. State Environmental Protection Administration, Beijing, China. **37** (03), 38, **2021**.
16. SALEM Z., GHOBARA M., NAHRAWY A.E. Spatio-temporal evaluation of the surface water quality in the middle Nile Delta using Palmer's algal pollution index. *Egyptian Journal of Basic & Applied Sciences*. **4** (3), 219, **2017**.
17. A BMP., A NS., A GGL., A MAM., B SP., A MS., A CTS., C TV., C PB., A AL. Consequences of eutrophication in the management of water resources in Mediterranean reservoirs: A case study of Lake Cedrino (Sardinia, Italy). *Global Ecology and Conservation*. **12** (C), 21, **2017**.
18. URIBE N., SRINIVASAN R., CORZO G., ARANGO D., SOLOMATINE D. Spatio-temporal critical source area patterns of runoff pollution from agricultural practices in the Colombian Andes. *Ecological Engineering*. **149**, 105810, **2020**.
19. WU L., LIU X., MA XY. Spatio-temporal variation of erosion-type non-point source pollution in a small watershed of hilly and gully region, Chinese Loess Plateau. *Environmental Science & Pollution Research*. **23** (11), 10957, **2016**.
20. XU H.S., XU Z.X., WU W., TANG F.F. Assessment and Spatiotemporal Variation Analysis of Water Quality in the Zhangweinan River Basin, China. *Procedia Environmental Sciences*. **13** (3), 1641, **2012**.
21. NIELSEN E.S. Growth of plankton algae as a function of N-concentration, measured by means of batch technique. *Marine Biology*. **46** (3), 185, **1978**.
22. JIANG P., LIU X., ZHANG J., SHU H.T., SHOEMAKER C.A. Cyanobacterial risk prevention under global warming using an extended Bayesian network. *Journal of Cleaner Production*. **312** (2), 127729, **2021**.
23. HUANG J., XU Q., WANG X., JI H., QUIGLEY EJ., SHARBATMALEKI M., LI S., XI B., SUN B., LI C. Effects of hydrological and climatic variables on cyanobacterial blooms in four large shallow lakes fed by the Yangtze River. *Environmental Science & Ecotechnology*. **5v** (159), 100069, **2021**.
24. HAMILTON PB., LAVOIE I., LEY LM., POULIN M. Factors contributing to the spatial and temporal variability of phytoplankton communities in the Rideau River (Ontario, Canada). *River Systems: Integrating landscapes, catchment perspectives, ecology, management*. **19** (3), 189, **2011**.
25. ZHANG Q., CHEN Y., WANG M., ZHANG J., LIU D. Molecular responses to inorganic and organic phosphorus sources in the growth and toxin formation of *Microcystis aeruginosa*. *Water Research*. **196** (1), 117048, **2021**.
26. HUDSON N., BAKER A., WARD D., REYNOLDS DM., BRUNSDON C., CARLIELL-MARQUET C., BROWNING S. Can fluorescence spectrometry be used as a surrogate for the Biochemical Oxygen Demand (BOD) test in water quality assessment? An example from South West England. *Science of the Total Environment*. **391** (1), 149, **2008**.
27. LIU Q., GUI Z., XIONG S., ZHAN M. A principal component analysis dominance mechanism based many-objective scheduling optimization. *Applied Soft Computing*. **113** (B), 107931, **2021**.
28. DING J., CAO J., XU Q., XI B., SU J., GAO R., HUO S., LIU H. Spatial heterogeneity of lake eutrophication caused by physiogeographic conditions: An analysis of 143 lakes in China. *Journal of Environmental Sciences*. **30** (04), 140, **2015**.
29. KARIMI AM., SADEGHNEJAD S., REZGHI M. Well-to-well correlation and identifying lithological boundaries by principal component analysis of well-logs. *Computers & Geosciences*. **157** (12), 104942, **2021**.
30. SCHMIDT H., KAUFMANN J., TONARIYA Y. Modeling end-users' acceptance of a knowledge authoring tool. *Methods of Information in Medicine*. **45** (05), 528, **2006**.
31. XIA C. Imbalance of plankton community metabolism in eutrophic Lake Taihu, China. *Journal of Great Lakes Research*. **37** (4), 650, **2011**.
32. WANG C. Effects of submerged macrophytes on sediment suspension and $\text{NH}_4\text{-N}$ release under hydrodynamic conditions. *Journal of Hydrodynamics, Ser B*. **22** (6), 810, **2010**.
33. LI M., HE H., MI T., ZHEN Y. Spatiotemporal dynamics of ammonia-oxidizing archaea and bacteria contributing

- to nitrification in sediments from Bohai Sea and South Yellow Sea, China. *Science of The Total Environment*. **825**, 153972, **2022**.
34. KHALIL S., MAHNASHI MH., HUSSAIN M., ZAFAR N., IRFAN M. Exploration and Determination of Algal Role as Bioindicator to Evaluate Water Quality – Probing Fresh Water Algae. *Saudi Journal of Biological Sciences*. **28** (10), 5728, **2021**.
 35. ZHANG Y., DOU M., LI P., LIANG Z., DAI P. Spatiotemporal variation characteristics and source identification of water pollutants in Shayinghe River basin. *River Research and Applications*. **37** (8), 1089, **2020**.
 36. YWL A., MOP B., SGK B., SSK B., BK C., JIN Y., DL E., SANG H. Major controlling factors affecting spatiotemporal variation in the dissolved oxygen concentration in the eutrophic Masan Bay of Korea. *Regional Studies in Marine Science*. **46** (70), 101908, **2021**.
 37. MATULA E.E., NABITY J.A. Effects of stepwise changes in dissolved carbon dioxide concentrations on metabolic activity in *Chlorella* for spaceflight applications. *Life Sciences in Space Research*. **29** (5), 73, **2021**.
 38. ZHANG M., CHU E., XU M., GUO J., ZHANG Y. Temporal and spatial variation analysis on nutritive salt of Hongze Lake. *Environmental Engineering Research*. **20** (1), 19, **2015**.
 39. JIAO Y., YANG C., HE W., LIU W.X., XU F.L. The spatial distribution of phosphorus and their correlations in surface sediments and pore water in Lake Chaohu, China. *Environmental Science & Pollution Research International*. **25** (1), 1, **2018**.
 40. HUO D., GAN N., GENG R., CAO Q., SONG L., YU G., LI R. Cyanobacterial blooms in China: diversity, distribution, and cyanotoxins. *Harmful Algae*. **109** (1), 102106, **2020**.
 41. ZHAO F., ZHAN X., XU H., ZHU G., ZOU W., ZHU M., KANG L., GUO Y., ZHAO X., WANG Z. New insights into eutrophication management: Importance of temperature and water residence time. *Journal of Environmental Sciences*. **1** (1), 229, **2022**.
 42. BEL A., AT B., MP B. Macroalgae reveal nitrogen enrichment and elevated N:P ratios on the Belize Barrier Reef. *Marine Pollution Bulletin*. **171**, 112686, **2021**.
 43. XIN X., ZHANG H., LEI P., TANG W., LI K. Algal Blooms in the Middle and Lower Hanjiang River: Characteristics, Early Warning and Prevention. *Science of The Total Environment*. **706**, 135293, **2020**.
 44. BING L., SHUANG G., YLA C., KCB C., FAN Y. Metal-based adsorbents for water eutrophication remediation: A review of performances and mechanisms. *Environmental Research*. **212** (Pt B), 113353, **2022**.
 45. FENG Z., HAI XA., LK A., XZ A. Spatial and Seasonal Change in Algal Community Structure and its Interaction With Nutrient Dynamics in A Gravel-bed Urban River. *Journal of Hazardous Materials*. **425** (SI), 127775, **2021**.
 46. DONG LA., SY B., ZC A., TQ A., HDA C. Process-oriented estimation of column-integrated algal biomass in eutrophic lakes by MODIS/Aqua - ScienceDirect. *International Journal of Applied Earth Observation and Geoinformation*. **99**, 102312, **2021**.
 47. ARMIN G., INOMURA K. Modeled temperature dependencies of macromolecular allocation and elemental stoichiometry in phytoplankton - ScienceDirect. *Computational and Structural Biotechnology Journal*. **19**, 5421, **2021**.
 48. KNUTSON C.M., MCLAUGHLIN E.M., BARNEY B.M. Effect of temperature control on green algae grown under continuous culture. *Algal Research*. **35**, 301, **2018**.
 49. MONTAGNES D., FRANKLIN D.J. Effect of temperature on diatom volume, growth rate, and carbon and nitrogen content: Reconsidering some paradigms. *Limnology and Oceanography*. **46** (8), 2008, **2002**.
 50. IDE Y., MATSUKAWA Y., MIYASHIRO D., MAYAMA S., UMEMURA K. Unique observation method of temperature dependence of diatom floating by direct microscope. *Journal of Microbiological Methods*. **172**, 105901, **2020**.
 51. SOMMER U., GLIWICZ ZM., LAMPERT WL., DUNCAN A. The PEG-model of seasonal succession of planktonic events in fresh waters. *Archiv fur Hydrobiologie*. **106** (4), 433, **1986**.
 52. HL A., XIN LA., WX A., EAL B., BH A. Spatial and temporal variations of satellite-derived phytoplankton size classes using a three-component model bridged with temperature in Marginal Seas of the Western Pacific Ocean. *Progress in Oceanography*. **191** (SI), 102511, **2021**.
 53. LI B., WAN R., YANG G., WANG S., WAGNER P.D. Exploring the spatiotemporal water quality variations and their influencing factors in a large floodplain lake in China. *Ecological Indicators*. **115**, 106454, **2020**.
 54. TONG YA., XU XA., QI MA., SUN JA., ZHANG YA., ZHANG WB., WANG MA., WANG XC., ZHANG YD. Lake warming intensifies the seasonal pattern of internal nutrient cycling in the eutrophic lake and potential impacts on algal blooms. *Water Research*. **188** (1), 116570, **2020**.
 55. KRICHEN E., RAPAPORT A., FLOCH E.L., FOUILLAND E. A new kinetics model to predict the growth of micro-algae subjected to fluctuating availability of light. *Algal Research*. **58** (102362), **2021**.
 56. SINGH., S. P., PRIYANKA. Effect of temperature and light on the growth of algae species: A review. *Renewable & sustainable energy reviews*. **50**, 431, **2015**.
 57. RUBIO-ARIAS., CONTRERAS-CARAVEO., QUINTANA., RM., SAUCEDO-TERAN., RA., PINALES-MUNGUIA. An Overall Water Quality Index (WQI) for a Man-Made Aquatic Reservoir in Mexico. *INT J ENV RES PUB HE*. **9** (5), 1687, **2012**.
 58. ZHANG J., NI W., YANG L., STEVENSON RJ., QI J. Response of freshwater algae to water quality in Qinsan Lake within Taihu Watershed, China. *Physics & Chemistry of the Earth*. **36** (9-11), 360, **2011**.
 59. ZHANG H., GONG W., ZENG W., YAN Z., LIANG H. Organic carbon promotes algae proliferation in membrane-aeration based bacteria-algae symbiosis system (MA-BA). *Water Research*. **176** (1), 115736, **2020**.
 60. MO Y., OU L., LIN L., HUANG B. Temporal and spatial variations of alkaline phosphatase activity related to phosphorus status of phytoplankton in the East China Sea. *Science of The Total Environment*. **731** (4), 139192, **2020**.
 61. ZHANG H., ZONG R., HE H., LIU K., HUANG X. Biogeographic distribution patterns of algal community in different urban lakes in China: Insights into the dynamics and co-existence. *Journal of Environmental Sciences*. **100**, 216, **2021**.